

excitation by means of two harmonic forces  $F_0 e^{i\omega t}$ ,  $-F_0 e^{i\omega t}$  acting on two different points of the system provide the set of these response curves.

The ratios of these responses give us the information whether a nonlinear element lies between the points of excitation or not.

As an example let us look on the numerical experiment of the 3 DOF system (Fig. 3). The used excitation matrix is

$$F = \begin{pmatrix} 1 & 0 & 0 & -1 & -1 & 0 \\ 0 & 1 & 0 & 1 & 0 & -1 \\ 0 & 0 & 1 & 0 & 1 & 1 \end{pmatrix} = [F_1, F_2, F_3, F_4, F_5, F_6].$$

By means of the excitation under the first three columns we can judge that the nonlinear element does not lie parallel to spring  $K_1, K_4, K_5$ , i.e. that the nonlinearity is internal. The last triad of vectors  $F_4 \div F_6$  enables us to identify the internal nonlinearity.

As an example there are plotted on the Fig. 4 the response curves  $D_{14} = a_{14}/F_0$ ,  $D_{24} = a_{24}/F_0$  and  $D_{34} = a_{34}/F_0$ . The index 4 means, that the system is excited by the force vector  $F_4$  acting on points 1 and 2:  $F = F_0 \cdot F_4 = F_0[-1, 1, 0]^T$ ,  $F_0 = 1$ . Ratios  $D_{14}/D_{34}$ ,  $D_{24}/D_{34}$  and similarly  $D_{16}/D_{36}$ ,  $D_{26}/D_{36}$  for  $F_6$  are plotted in Figs. 5 and 6 for two amplitudes of the exciting forces  $F_0 = 1$  and  $F_0 = 2$ .

In Fig. 5 the curves are singlevalued and do not depend either on the amplitude of vibrations or on the amplitude of excitation. Fig. 6 shows the large dependence on the force amplitude and the curves are in some interval multiple valued.

Comparing both Figures it is evident, that the nonlinear element is situated between the points 1 and 2.

## Reference

1 PŮST, L.: Identification of position and characteristics of nonlinear element in the vibrating system. Euromech 280 Symposium on identification of nonlinear mechanical systems, October 1991, ECL, Lyon, France.

Address: Ing. L. PŮST, DrSc., Institute of Thermomechanics, Dolejškova 5, 18200 Praha 8, Czech Republic

ZAMM · Z. angew. Math. Mech. 73 (1993) 4–5, T 87–T 91

Akademie Verlag

SÖFFKER, D.; BAJKOWSKI, J.; MÜLLER, P. C.

## Analysis and Detection of the Cracked Rotor

MSC (1980): 73M05, 62N05, 70J30

### 1. Formulation of the problem

It is very difficult to conclude the existence of a shaft crack in a rotor, because there is no clear relation between the crack and the caused phenomena. In this way the main problem is, to establish a clear and unambiguous relation between the crack and the caused phenomena.

Here a new method [1, 2, 3], based on the theory of disturbance rejection control is presented. In this way the crack is interpreted as an external disturbance. The nonlinear equations of motion for the rotating cracked shaft are described by

$$M\ddot{z} + (D + G)\dot{z} + Kz = f(t) + N_n h(z(t), t) \quad (1)$$

with  $z$ ,  $\dot{z}$ ,  $\ddot{z}$  the displacement vector and its time derivatives of order  $n$ ,  $M$  the mass matrix,  $D$ ,  $G$  the matrices of damping and gyroscopic effects,  $K$  the stiffness matrix,  $f(t)$  the vector of unbalances,  $N_n$  the input matrix of nonlinearities, and  $h(z(t), t)$  the vector of nonlinearities caused by the crack.

The vector  $h(z(t), t)$  contains the specific forces caused by the crack. To consider the crack influences in the equations of motion (1) a crack model is needed in the way that it describes the change in stiffness and/or damping coefficients e.g. by a crack element stiffness [4, 5] or damping matrix.

The simple crack model of GASCH, Fig. 1, is described in the rotating coordinate system by

$$\begin{bmatrix} \xi \\ \eta \end{bmatrix} = \begin{bmatrix} h + h_a & 0 \\ 0 & h \end{bmatrix} \begin{bmatrix} F_\xi \\ F_\eta \end{bmatrix}. \quad (2)$$

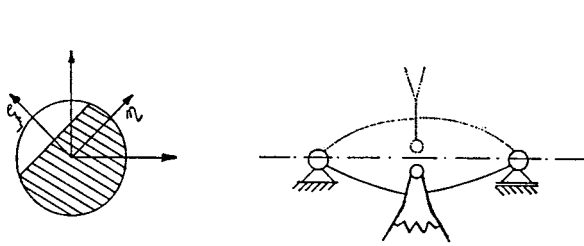


Fig. 1. Illustration of the crack model of GASCH [4]

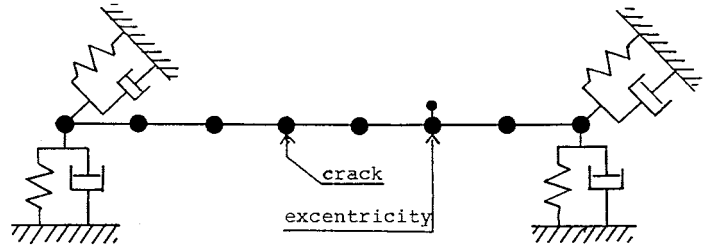


Fig. 2. Simple rotor

The compliance  $h$  in crack direction  $\xi$  will be increased with an additional compliance  $h_a$  in case of an open crack which depends on the crack depth. The relative crack compliance  $h_r$  as the ratio

$$h_r = h_a/h \quad (3)$$

is established by experimental investigations of MAYES and DAVIES [6] for different crack depths. For very small cracks the values are approximated. The opening-condition of the crack can be formulated via the curvature at crack position, or approximately via the displacements near the crack, cf. [10]. The element-stiffness-matrix  $K_e(\ddot{z}(t), t)$  for a discretized model like an MBS-formulation in the inertial coordinate system looks like

$$K_e = \frac{-h_r}{h(1+h_r)} \begin{bmatrix} \sin^2(\Omega t + \beta) & \sin(\Omega t + \beta) \cos(\Omega t + \beta) \\ \sin(\Omega t + \beta) \cos(\Omega t + \beta) & \cos^2(\Omega t + \beta) \end{bmatrix}, \quad (4)$$

where  $K_e$  depends on the opening condition for the crack and on time, so the system in inertial coordinates becomes a nonlinear and parameter excited one.

## 2. Behaviour of the cracked rotor

There exist several quantitative and qualitative measures for the characterization of the system behaviour (attractors), e.g. such of phase plane plots, Poincaré sections, FFT-analysis, different kinds of dimensions and entropies [7]. Lyapunov exponents are chosen here to classify the system behaviour. For periodic attractors one obtains only negative and zero exponents indicating convergence to a highly predictable motion, whereas a chaotic system will exhibit at least one positive exponent. A positive exponent is significant because it gives an indication of the rate at which one loses the ability to predict the system response. This is closely tied to the property of sensitive dependence on initial conditions which is present in chaotic systems. Therefore, one way to determine if a system is behaving in a chaotic manner is to calculate the Lyapunov exponents. The rotor used for theoretical investigations and simulations is described by the following assumptions (cf. Fig. 2): Rotor as a lumped-mass-model: 7 beam elements, length  $l = 600$  mm; radius  $r = 140$  mm; frequency  $\Omega = 100\pi$  rad/s; excentricity  $e_m = 0.02$  mm; stiffness of bearings  $k_s = 750$  kN/mm; damping as  $D = \alpha_{\text{mod}}M + \beta_{\text{mod}}K$ ,  $\alpha_{\text{mod}} = 0$ ,  $\beta_{\text{mod}} = 0.00001$ ; number of degrees of freedom  $n = 16$ ; number of nonlinearities  $f = 2$ ; number of measurements  $m = 8$  (measurements only in bearings as displacements and their velocities).

The Lyapunov exponents were calculated by making use of the algorithms given in [8]. To implement this procedure the fiducial trajectory is created by integrating the nonlinear equations of motion for some post-transient initial conditions (here 32 differential equations). Simultaneously, the linearized equations of motion, here nondifferentiable dynamic system – piecewise linear and parameter excited one – with transition-matrix according to [9] and transition conditions given in [10], are integrated for  $2n$  different initial conditions (here  $32 \times 32 = 1024$  differential equations), defining an arbitrarily oriented frame of  $2n$  orthonormal vectors. Because of the order of the system,  $(32 + 1024)$ , only the greatest Lyapunov exponent  $\sigma_1$  was calculated as a function of relative crack compliance  $h_r$ . The results are shown in Fig. 3a.

As the crack coefficient  $h_r$  is varied, different types of motion are observed, Figs. 3b, c. For certain regions in the parameter space, as the parameter  $h_r$  is varied, the periodic motions become unstable and bifurcate giving rise to stable quasiperiodic motions, Fig. 3b (point 1,  $h_r = 0.1032$  in Fig. 3a). For certain values of  $h_r$  these almost periodic motions (or periodic motions) become unstable and bifurcate giving rise to stable chaotic motions, Fig. 3c (point 2,  $h_r = 0.108$  in Fig. 3a).

## 3. State observers for reconstruction of nonlinear effects

Applying state space notation equation (1) is described by

$$\dot{x} = Ax + b(t) + Nn(x(t)), \quad y = Cx. \quad (5)$$

Here  $x$  denotes the  $2n$ -dimensional state vector,  $A$  is the  $2n \times 2n$  system matrix,  $b$  represents the  $2n$ -dimensional vector of control inputs and/or excitation functions. The  $2n \times f$  matrix  $N$  is the input matrix of the nonlinearities into the linear

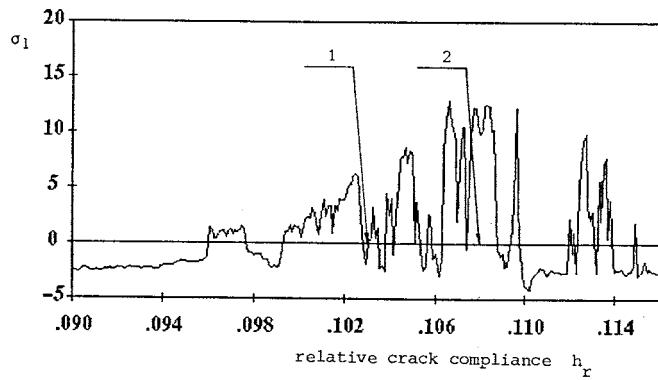


Fig. 3a. Greatest Lyapunov exponent as a function of relative crack compliance for constant damping coefficient  $\beta_{\text{mod}} = 0.00001$  (after WOLF et al. [8])

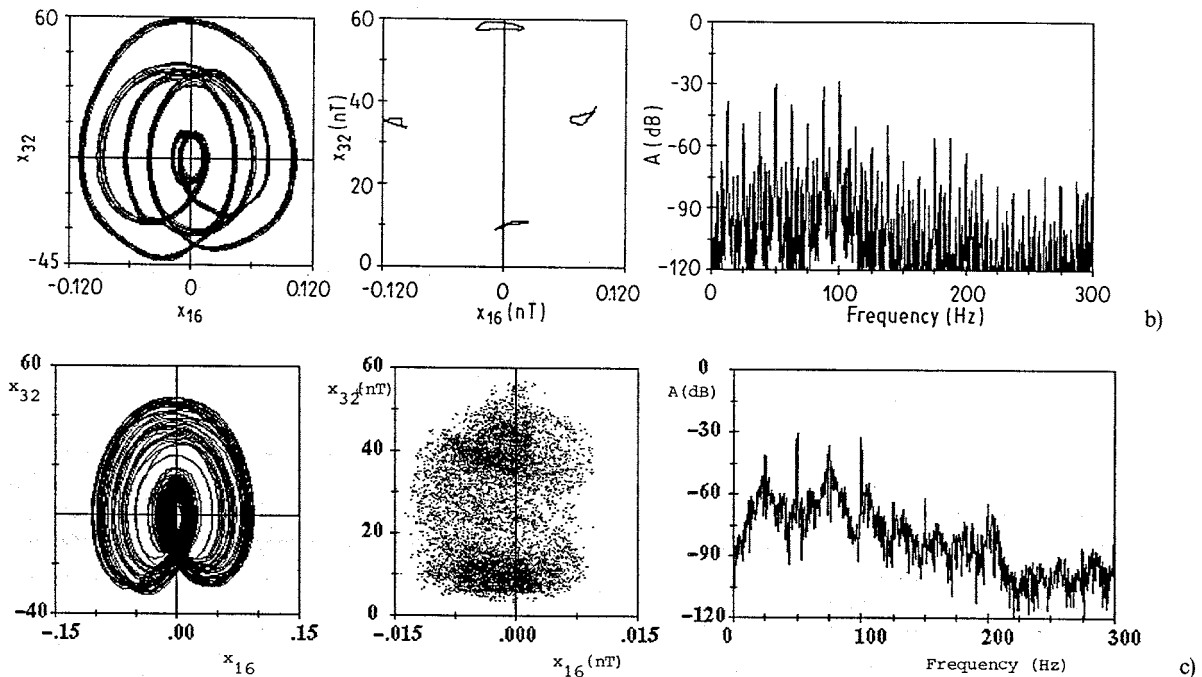


Fig. 3b, c. Projection onto the  $(x_{16}, x_{32})$  plane (right bearing, horizontal direction) of the trajectory, Poincaré map with  $t_0 = 0$ ;  $T = 2\pi/\Omega$ ,  $\Omega = 50$  Hz,  $n = 10000$ ); and corresponding power spectrum ( $A = 20 \log \sqrt{\text{Im}_{16}^2 + \text{Re}_{16}^2}$ ), for different relative crack compliance  $h_r$ , [b]  $h_r = 0.1032$ , c)  $h_r = 0.108$ ] and constant damping coefficient  $\beta_{\text{mod}} = 0.00001$

dynamical system. The vector  $n(x(t), t)$  characterizes the  $f$ -dimensional vector of nonlinear functions. The  $m$ -dimensional vector  $y$  represents the measurements via the  $m \times 2n$ -dimensional matrix of measurements  $C$ . It is assumed that the system parameters ( $A, N, C$ ) as well as the input and output time signals ( $b, y$ ) are known. The task is to reconstruct the unknown nonlinearities (here the external disturbance forces of the crack)

$$n(x(t), t) \approx \hat{n}(\hat{x}(t)) \quad (6)$$

by applying state observers. For consideration of external disturbances, the state space vector should be extended by a fictitious disturbance vector  $v(t)$ ,

$$n(x(t)) \approx H v(t), \quad \dot{v}(t) = F v(t) + G b(t), \quad \dim v = s, \quad (7)$$

to describe approximately the time behaviour of the nonlinearities [2]. The model matrices  $F, H$  and  $G$  must be chosen in accordance with the technical background about the system. Here  $NH$  couples the fictitious model (7) to the whole system. The matrices are of  $N[2n, f]$ ,  $H[f, (r_{ni} \cdot f)]$ ,  $F[r_{ni} \cdot f, r_{ni} \cdot f]$ ,  $r_{ni} = 2$ , order.

In this way the external forces caused by the crack are reconstructed by the estimates of the disturbance vector  $v(t)$  as  $\hat{v}(t)$ . Applying (7) the extended system is obtained with the new system matrix  $A_e$ ,

$$\begin{bmatrix} \dot{\hat{x}}(t) \\ \dot{\hat{v}}(t) \end{bmatrix} = \underbrace{\begin{bmatrix} A & NH \\ \mathbf{0} & F \end{bmatrix}}_{A_e} \begin{bmatrix} x(t) \\ v(t) \end{bmatrix} + \begin{bmatrix} I \\ G \end{bmatrix} b(t), \quad y(t) = [C \ 0] \begin{bmatrix} x(t) \\ v(t) \end{bmatrix} + \begin{bmatrix} w(t) \\ \mathbf{0}(t) \end{bmatrix}, \quad (8)$$

where  $w(t)$  represents state measurement noise. The noise vector  $w(t)$  is assumed to be zero-mean, white random sequence. This extended system (8) with the new system matrix  $A_e$  could be observed by the extended state space observer if the system is completely observable [11]. This requires a suitable choice of matrices  $F, H$  and  $G$  and measurements [1, 3].

The reconstruction of the characteristic relative crack compliance  $h_r$ , cf. (3), can be done by simple calculations using the transformation matrix, the estimated disturbance forces  $\hat{v}(t)$ , estimated displacements at crack position and phase information  $\beta$ .

The gain matrices of the observer can be chosen by: a) the pole assignment method or b) a Riccati observer, which fulfills the following requirements:

$$A_e P + P A_e^T - P C^T R^{-1} C P + Q = 0. \tag{9}$$

Since using approximations instead of the real nonlinearities the weighting matrices  $R$  and  $Q$  must be chosen specifically [10],

$$Q = \begin{bmatrix} q_1 I_n & 0 & 0 \\ 0 & q_2 I_n & 0 \\ 0 & 0 & q_3 I_{r,n,f} \end{bmatrix}, \quad R = r I_m. \tag{10}$$

#### 4. Crack detection by state observers

Crack detection by state observers means a procedure with two steps:

1. Estimation of crack forces  $\hat{v}(t)$  via the extended state space observer.
2. Recalculating the coefficients of  $K_e(\tilde{z}(t), t)$  (4) or e.g.  $h_a(t)$  (3) for each time step and representing them in a favourable manner, e.g. dividing by the nominal values of the undamaged case.

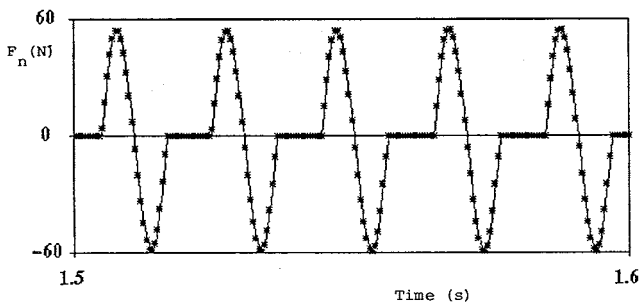


Fig. 4a) Reconstructed horizontal crack forces  $\hat{v}$  ( $t_r = 10\%$ )

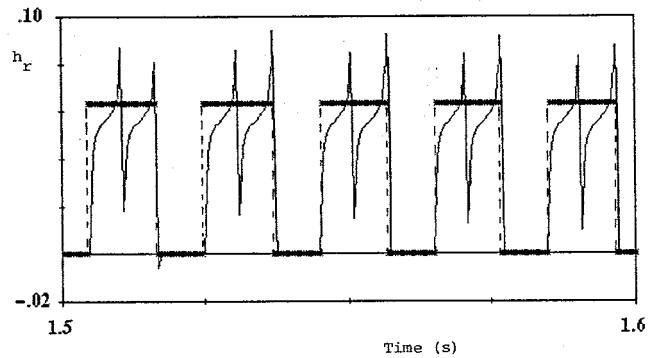


Fig. 4b) Recalculated relative crack compliance  $h_r$ ; using a Riccati observer

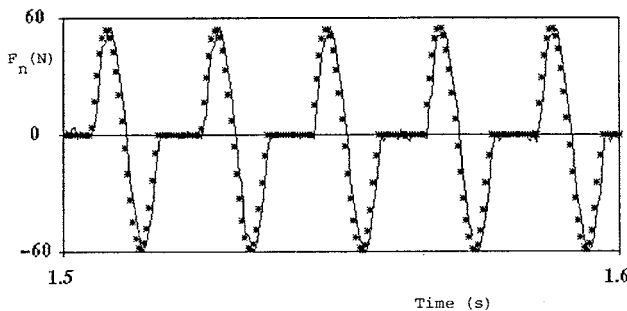


Fig. 4c) Reconstructed horizontal crack forces  $\hat{v}$  ( $t_r = 10\%$ )

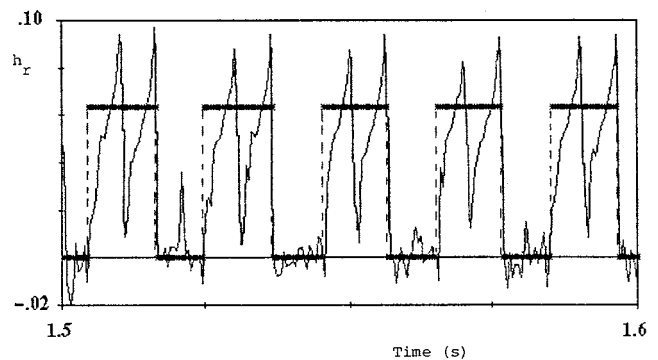


Fig. 4d) Recalculated relative crack compliance  $h_r$ , with S/N 26 dB ratio in measurements, using Riccati observer

(\*\*\*\*\* simulation result, ——— reconstruction/recalculation)

Figs. 4a, b show the disturbance force caused by crack  $F_n$  in horizontal direction and relative crack compliance  $h_r$  for crack depth  $t_r = 10\%$ , using a Riccati observer with  $q_1 = 1$ ,  $q_2 = 1$ ,  $q_3 = 10^9$  and  $r = 0.001$ .

In the case it was noticed that elements of the gain matrices were too large, the observer became sensitive with respect to noisy measurements. Therefore, to generate measurement signals with 26 dB signal to noise (S/N) ratio, we have applied a Riccati observer with  $q_1 = q_2 = 1$ ,  $q_3 = 300$  and  $r = 0.01$ . The results are shown in Figs. 4c, d.

The observer estimates the signal very well. The external signal only exists if the crack opens, the maximal values depend on the crack depth (Figs. 4a, c). Using this estimation and the estimation about the displacements the normally unknown ratio  $h_r = h_o/h$  in (3) can be recalculated, Figs. 4b, d. As a function of time this ratio describes the variable compliance or stiffness depending on the phase angle in the rotating coordinate system. Hence it will be a clear indicator for cracks. Here the opening and closing of the crack is shown very clear and unambiguous. For crack depth of 10% of radius it is very clear to see: opening and closing of the crack in the crack model of GASCH. Using other crack models leads to the reconstruction of the accompanying relative crack compliance function. In contrast to this the calculations of an undamaged rotor result in a ratio about 0.001.

## 5. Summary

The vibrational behaviour of a cracked rotating shaft is an important problem for engineers working in the area of the dynamics of machines. An early warning can considerably extend the durability of these machines increasing their reliability at the same time.

To examine the behaviour of the system beside phase plane plots, Poincaré maps, time histories and power spectrum, the linearized equations of motion and transition conditions were obtained and the Lyapunov exponent was calculated.

The main problem in crack detection is to establish a clear and unambiguous relation between the crack and the caused phenomena which can be measured only in bearings.

Therefore a new observer-based method has been developed and applied to a turbo-rotor. This method gives a clear relation between shaft cracks and caused phenomena in vibrations measured in bearings. Simulations have been done, showing the success of this method, especially for reconstructing disturbance forces as inner forces caused by a crack. Calculating the relative crack compliance as the ratio of additional compliance caused by the crack and undamaged compliance a clear statement about the opening and closing, and therefore for the existence of the crack, and about the crack depth is possible. Theoretically it has been shown that it is possible to detect a crack with very small stiffness changes which corresponds to a crack depth of 10% of the radius of the rotor. The results are nearly the same if noisy measurements are considered.

## References

- 1 SÖFFKER, D.; BAJKOWSKI, J.: Crack detection by state observers. In: Proc. 8th IFToMM World Congress on the Theory and Practice of Machines and Mechanism, Prague 1991, pp. 771–774.
- 2 MÜLLER, P. C.: Indirect measurements of nonlinear effects by state observers. In SCHIEHLEN, W. (eds.): IUTAM Sympos. on Nonlin. Dynamics in Engineering Systems. University of Stuttgart, Springer-Verlag, Berlin 1990, pp. 205–215.
- 3 SÖFFKER, D.; BAJKOWSKI, J.; MÜLLER, P. C.: Detection of cracks in turbo rotors – a new observer based method. J. Dynamic Systems, Measurements and Control, June 1993 (to appear).
- 4 GASCH, R.: Dynamic behaviour of a simple rotor with a cross-sectional crack. In: Vibrations in rotating machinery. Institution of Mechanical Engineers, London 1976, pp. 123–128.
- 5 SCHMALHORST, B.: Experimentelle und theoretische Untersuchungen zum Schwingungsverhalten angerissener Rotoren. VDI-Fortschrittsberichte Nr. 117, Reihe 11, VDI-Verlag, Düsseldorf 1989.
- 6 MAYES, I. W.; DAVIES, W. G. R.: Analysis of the response of a multi-rotor-bearing system containing a transverse crack in a rotor. J. Vibration, Acoustics, Stress and Reliability in Design, 1984, pp. 139–145.
- 7 MOON, F. C.: Chaotic vibrations, an introduction for applied scientists and engineers. Wiley, New York 1987.
- 8 WOLF, A.; SWIFT, J. B.; SWINNEY, H. L.; VASTANO, J. A.: Determining Lyapunov exponents from a time series. Physica D 16 (1985), 285–317.
- 9 MÜLLER, P. C.; BAJKOWSKI, J.; KISLJAKOV, S. D.: Model based calculation of Lyapunov exponents for dynamic systems with discontinuities. In: 2nd Polish-German Workshop on Dynamical Problems in Mechanical Systems. March 10–17, Paderborn/Germany 1991.
- 10 MÜLLER, P. C.; BAJKOWSKI, J.; SÖFFKER, D.: Chaotic motions and fault detection in a cracked rotor. Dynamics, 1993 (to appear).
- 11 LUENBERGER, D. G.: An introduction to observers. IEEE Trans. Automatic Control AC-16 (1971), 596–602.

Addresses: Dipl.-Ing. DIRK SÖFFKER, Dr.-Ing. JOZEF BAJKOWSKI, Prof. Dr. rer. nat. PETER C. MÜLLER, Bergische Universität – GH Wuppertal, Sicherheitstechnische Regelungs- und Meßtechnik, Gaußstraße 20, D-W-5600 Wuppertal 1, Germany